

# Recurrent *de novo* missense variants across multiple histone H4 genes underlie a neurodevelopmental syndrome

Federico Tessadori,<sup>1</sup> Karen Duran,<sup>2</sup> Karen Knapp,<sup>3</sup> Matthias Fellner,<sup>3</sup> Deciphering Developmental Disorders Study, Sarah Smithson,<sup>4</sup> Ana Beleza Meireles,<sup>4</sup> Mariet W Elting,<sup>5</sup> Quinten Waisfisz,<sup>5</sup> Anne O'Donnell-Luria,<sup>6,7,8</sup> Catherine Nowak,<sup>8</sup> Jessica Douglas,<sup>8</sup> Anne Ronan,<sup>9</sup> Theresa Brunet,<sup>10,11</sup> Urania Kotzaeridou,<sup>12</sup> Shayna Svihovec,<sup>13</sup> Margarita S Saenz,<sup>13</sup> Isabelle Thiffault,<sup>14,15,16</sup> Florencia Del Viso,<sup>15,16</sup> Patrick Devine,<sup>17</sup> Shannon Rego,<sup>17</sup> Jessica Tenney,<sup>18</sup> Arie van Haeringen,<sup>19</sup> Claudia AL Ruivenkamp,<sup>19</sup> Saskia Koene,<sup>19</sup> Stephen P Robertson,<sup>20</sup> Charulata Deshpande,<sup>21</sup> Rolph Pfundt,<sup>22</sup> Nienke Verbeek,<sup>23</sup> Jiddeke M van de Kamp,<sup>7</sup> Janneke MM Weiss,<sup>7,22</sup> Anna Ruiz,<sup>24</sup> Elisabeth Gabau,<sup>25</sup> Ehud Banne,<sup>26</sup> Alexander Pepler,<sup>27</sup> Armand Bottani,<sup>28</sup> Sacha Laurent,<sup>29</sup> Michel Guipponi,<sup>29</sup> Emilia Bijlsma,<sup>19</sup> Ange-Line Bruel,<sup>30,31</sup> Arthur Sorlin,<sup>32</sup> Mary Willis,<sup>33</sup> Zoe Powis,<sup>34</sup> Thomas Smol,<sup>35</sup> Catherine Vincent-Delorme,<sup>36</sup> Diana Baralle,<sup>37</sup> Estelle Colin,<sup>38</sup> Nicole Revencu,<sup>39</sup> Eduardo Calpena,<sup>40</sup> Andrew OM Wilkie,<sup>40</sup> Maya Chopra,<sup>41</sup> Valerie Cormier-Daire,<sup>42</sup> Boris Keren,<sup>43</sup> Alexandra Afenjar,<sup>44</sup> Marcello Niceta,<sup>45</sup> Alessandra Terracciano,<sup>46</sup> Nicola Specchio,<sup>47</sup> Marco Tartaglia,<sup>45</sup> Marlene Rio,<sup>48</sup> Giulia Barcia,<sup>48</sup> Sophie Rondeau,<sup>48</sup> Cindy Colson,<sup>49</sup> Jeroen Bakkers<sup>1,50</sup>, Peter D Mace,<sup>3</sup> Louise S Bicknell,<sup>3#</sup> Gijs van Haaften,<sup>2#</sup>.

1. Hubrecht Institute-KNAW and University Medical Center Utrecht, Uppsalalaan 8, 3584 CT Utrecht, the Netherlands.
2. Department of Genetics, Center for Molecular Medicine, University Medical Center Utrecht, Utrecht University, 3584 CX Utrecht, the Netherlands.
3. Department of Biochemistry, University of Otago, Dunedin 9016, New Zealand.
4. Bristol Regional Genetics Service, University Hospitals Bristol and Weston NHS Foundation Trust, Bristol, BS2 8EG, UK.

5. Amsterdam UMC, Afdeling Klinische genetica, 1081 HV Amsterdam, the Netherlands.
6. Program in Medical and Population Genetics, Broad Institute of MIT and Harvard, Cambridge, Massachusetts 02142, USA.
7. Division of Genetics and Genomics, Boston Children's Hospital, Boston, Massachusetts 02115, USA.
8. Manton Center for Orphan Disease Research, Boston Children's Hospital, Boston, Massachusetts 02115, USA.
9. Clinical Genetics, Hunter Genetics Unit, Waratah NSW 2298, Australia.
10. Institute of Medical Genetics, 81675 Munchen, Germany.
11. Institute of Neurogenomics, Helmholtz Zentrum München, 85764 Neuherberg, Germany.
12. Division of Child Neurology and Inherited Metabolic Diseases, Department of Pediatrics, Heidelberg University Hospital, 69120 Heidelberg, Germany.
13. Section of Genetics and Metabolism, Department of Pediatrics, The Children's Hospital Colorado, University of Colorado Anschutz Medical Campus, Aurora, Colorado 80045, USA.
14. University of Missouri-Kansas City School of Medicine, Kansas City, Missouri 64108, USA.
15. Center for Genomic Medicine, Children's Mercy Research Institute, Kansas City, Missouri 64108, USA.
16. Department of Pathology and Laboratory Medicine, Children's Mercy Hospital, Kansas City, Missouri 64108, USA.
17. Institute for Human Genetics, University of California, San Francisco, California 94143, USA.
18. Division of Medical Genetics, Department of Pediatrics, University of California, San Francisco, California 94143, USA.

19. Department of Clinical Genetics, Leiden University Medical Center, 2333 ZA Leiden, the Netherlands.
20. Department of Women's and Children's Health, Dunedin School of Medicine, University of Otago, Dunedin 9016, New Zealand.
21. Guy's and St Thomas' NHS Foundation Trust, London SE1 9RT, UK.
22. Department of Human Genetics, Radboud University Medical Centre, 6500 HB Nijmegen, the Netherlands.
23. Department of Genetics, University Medical Centre Utrecht, 3584 CX Utrecht, the Netherlands.
24. Genetics Laboratory, UDIAT-Centre Diagnòstic. Parc Taulí Hospital Universitari. Institut d'Investigació i Innovació Parc Taulí I3PT. Universitat Autònoma de Barcelona. 08208 Sabadell, Spain.
25. Paediatric Unit, Parc Taulí Hospital Universitari, Institut d'Investigació i Innovació Parc Taulí I3PT, Universitat Autònoma de Barcelona, 08208 Sabadell, Barcelona, Spain.
26. Kaplan Medical Center, Clalit Health Services, Rehovot 76100, Israel.
27. Praxis für Humangenetik Tübingen, 72076 Tuebingen, Germany.
28. Service of Genetic Medicine, Geneva University Hospitals, 1205 Geneva, Switzerland.
29. Department of Genetic Medicine, University Hospitals of Geneva & University of Geneva Medical Faculty, Geneva 1211, Switzerland.
30. UMR1231 GAD, Inserm – Université Bourgogne-Franche Comté, 21078 Dijon, France.
31. Centre de référence Déficiences Intellectuelles de Causes Rares, Dijon Bourgogne University Hospital, 21079 Dijon, France.
32. Centre de Référence maladies rares « Anomalies du développement et syndromes malformatifs », centre de génétique, FHU-TRANSLAD, Dijon Bourgogne University Hospital, 21079 Dijon, France.

- 83 33. Department of Pediatrics, Naval Medical Center San Diego, San Diego, California  
84 92134, USA.
- 85 34. Ambry Genetics, California 92656, USA.
- 86 35. Univ. Lille, RADEME EA7364, CHU Lille, Institut de Génétique Médicale, F-59000  
87 Lille, France.
- 88 36. Department of Clinical Genetics, CHU Lille, F-59000 Lille, France.
- 89 37. Faculty of Medicine, University of Southampton, Southampton SO16 6YD, UK.
- 90 38. Department of Biochemistry and Genetics, University Hospital, F-49933 Angers,  
91 France.
- 92 39. Center for Human Genetics, Cliniques universitaires Saint-Luc, Université catholique  
93 de Louvain, 1200 Brussels, Belgium.
- 94 40. MRC Weatherall Institute of Molecular Medicine, University of Oxford, John Radcliffe  
95 Hospital, Oxford OX3 9DS, UK.
- 96 41. Rosamund Stone Zander Translational Neuroscience Center, Boston Children's  
97 Hospital, Boston MA 021115, USA.
- 98 42. Université de Paris, Department of Clinical Genetics and Reference Centre for  
99 Constitutional Bone Diseases, INSERM U1163, Imagine Institute, Necker-Enfants  
100 Malades Hospital, AP-HP, 75015 Paris, France.
- 101 43. Genetic Department, APHP, Sorbonne Université, Pitié-Salpêtrière Hospital, 47-83  
102 Boulevard de l'Hôpital, 75013 Paris, France.
- 103 44. CRMR malformations et maladies congénitales du cervelet et déficiences  
104 intellectuelles de causes rares, Département de génétique, Sorbonne Université, AP-  
105 HP, Hôpital Trousseau, 75012 Paris, France.
- 106 45. Area di Ricerca Genetica e Malattie Rare, Ospedale Pediatrico Bambino Gesù,  
107 IRCCS, 00146 Rome, Italy.
- 108 46. Area di Ricerca Medicina Multimodale di Laboratorio, Ospedale Pediatrico Bambino  
109 Gesù, IRCCS, 00146 Rome, Italy.



47. Area di Ricerca Scienze Neurologiche e Medicina Riabilitativa, Ospedale Pediatrico Bambino Gesù, IRCCS, 00163 Rome, Italy.
48. Department of Genetics, Necker Enfants Malades Hospital, Paris Descartes-Sorbonne Paris Cité University, 75015 Paris, France.
49. CHU Lille, Clinique de Génétique, 59000, Lille, France.
50. Department of Pediatric Cardiology, Division of Pediatrics, University Medical Center Utrecht, 3584 CX Utrecht, the Netherlands.

#Correspondence to: Louise Bicknell [louise.bicknell@otago.ac.nz](mailto:louise.bicknell@otago.ac.nz) or Gijs van Haften [G.vanHaften@umcutrecht.nl](mailto:G.vanHaften@umcutrecht.nl)

## Summary

Chromatin is essentially an array of nucleosomes, each of which consists of the DNA double-stranded fiber wrapped around a histone octamer. This organization supports cellular processes like DNA replication, DNA transcription and DNA repair in all eukaryotes. Human histone H4 is encoded by fourteen canonical histone H4 genes, all differing at the nucleotide level but encoding an invariant protein. Here we present a cohort of 29 subjects with *de novo* missense variants in six H4 genes (*H4C3*, *H4C4*, *H4C5*, *H4C6*, *H4C9* and *H4C11*) identified by whole exome sequencing and matchmaking. All individuals present with neurodevelopmental features of intellectual disability and motor and/or gross developmental delay, while non-neurological features are more variable. Ten amino acids are affected, six of which recurrently, and are all located within the H4 core or C-terminal tail. These variants cluster to specific regions of the core H4 globular domain, where protein-protein interactions occur with either other histone subunits or histone chaperones. Functional consequences of the identified variants were evaluated in zebrafish embryos, which displayed abnormal general development, defective head organs and reduced body axis length, providing compelling evidence for the causality of the reported disorder(s). While multiple

developmental syndromes have been linked to chromatin-associated factors, missense-bearing histone variants (e.g. H3 oncohistones) are only recently emerging as a major cause of pathogenicity. Our findings establish a broader involvement of H4 variants in developmental syndromes.

Histones are amongst the most slowly evolving genes in eukaryotes.<sup>1,2</sup> Histone H4 acts as a functional unit by forming a dimer with H3, but unlike H3 there are no variant isoforms linked to specific cellular processes. We previously reported four individuals with a primordial dwarfism phenotype with *de novo* missense variants affecting Lys91 in *H4C3*(*HIST1H4C*; MIM 602827) and *H4C11*(*HIST1H4J*; MIM 602826), a critical residue near the C-terminus of the protein prone to post-translational modifications (PTMs) such as acetylation<sup>3</sup>, or more important here, ubiquitination.<sup>4-6</sup> Somatic variation in H4 is potentially relevant in a cancer setting,<sup>7,8</sup> although described variation impacts multiple residues in contrast to the highly recurrent pathogenic variants observed for the established oncohistone, H3.<sup>8</sup> This could be reconducted to the fact that while the functional importance of PTMs on N-tails of H3 is linked to the chromatin effectors they correlate to<sup>9-11</sup>, variants affecting the histone core (H4 in this case) have more direct and global consequences on chromatin organization, as they impact nucleosome structure and dynamics.<sup>12</sup>

We have identified an additional cohort of 29 individuals with *de novo* missense variants in six different histone H4 genes: *H4C3* (*HIST1H4C*), *H4C4* (*HIST1H4D*; MIM 602823), *H4C5* (*HIST1H4E*; MIM 602830), *H4C6* (*HIST1H4F*; MIM 602824), *H4C9* (*HIST1H4I*; MIM 602833) and *H4C11* (*HIST1H4J*) (Figure 1A, Table 1). The cohort was collected using trio-based whole-exome sequencing in combination with data sharing via Genematcher<sup>13</sup> and DECIPHER.<sup>14</sup> This study received ethical approval from the New Zealand Health and Disability Ethics Committee (16/STH/3) and London–Riverside REC (09/H0706/20). All

families provided consent to be involved in this project, with separate consent obtained for the use of photos.

There are fourteen canonical *histone H4* genes in the human genome, clustering in three genomic loci. At a nucleotide level, all genes are different, but together they encode an identical protein. Transcription of these genes is independently regulated, with differing expression levels observed during brain development<sup>15,16</sup> and in human tissues.<sup>4</sup> The genes harboring variants identified in our cohort are amongst the more highly expressed, however as H4 transcripts are not polyadenylated and therefore missed in most RNAseq protocols, limited expression data is available.

All variants observed were absent from control databases (1KG, gnomAD v2.1.1).<sup>17</sup> Furthermore, there were no missense variants affecting Lys91 in any of the fourteen canonical histone H4 genes in gnomAD, and only extremely rarely were substitutions observed for the other positions in different H4 genes. The absence of any substitutions at Lys91 could reflect a stronger requirement for fidelity at this position, especially given the post-translation modifications of Lys91.<sup>18</sup>

The genetic findings of the cohort are striking, especially given that histones are some of the slowest evolving eukaryotic proteins and human H4 is 92% conserved with the yeast orthologue.<sup>1,2</sup> In the human population, the histone H4 genes are tolerant to both loss-of-function and missense variation (gnomAD). We identify nine sites across the 103 amino acid protein with a mutation, six of which were found recurrently (Pro32, Arg40, Arg45, His75, Lys91 and Tyr98), including two where the same site (Pro32 and Arg40) is mutated in multiple different H4 genes. All sites are conserved through to *Saccharomyces cerevisiae*. The mutated residues cluster in two main regions of histone H4 (Figure 1B); one cluster centers on the first  $\alpha$ -helix of H4 (Figure 1B; purple spheres), a region important for DNA contacts and protein interactions with H3 and histone chaperones.<sup>18</sup> Arg45 is positioned in the loop following the first  $\alpha$ -helix and forms one of the sprockets of the nucleosome which

contacts the minor groove of DNA. Substitutions at Arg45 in *Saccharomyces cerevisiae* have proven to be deleterious to growth and fitness with altered chromatin remodeling.<sup>7,19,20</sup> The second cluster is within the core of the nucleosome (Figure 1B, orange spheres), where important structural contacts exist between the H3-H4 dimer and with histone chaperones.<sup>18</sup> Suggestive evidence for these other variants also originates from *S. cerevisiae*, where a Gly94 mutant (a key residue for H4 C-terminal flexibility) confers reduced viability,<sup>21</sup> whereas a His75 mutant disrupts DNA damage repair processes.<sup>22</sup> Other studied variants in similar regions (either somatic ‘oncohistone’ variants in H4,<sup>7,8</sup> or recently described germline variants in H3<sup>23</sup>) are predicted to perturb either nucleosome stability or interaction with histone chaperones, suggesting the H4 variants described in our cohort likely cause similar effects. These complementary observations, alongside the significant recurrence of specific variants, provide strong evidence for pathogenicity.

All individuals displayed intellectual disability (ID) and the majority demonstrated global and/or gross motor developmental delay (Table 2, Table S1). Other neurodevelopmental features such as hypotonia (34%), seizures (17%) or autism (17%) were present in some individuals but less common. Brain MRI was generally normal except for two individuals with delayed myelination. Microcephaly was commonly observed (Figure 2A), with an occipitofrontal circumference Z-score smaller than -2 SD evident in 16% individuals at birth and becoming progressively more severe with age (76% at the most recent exam). Short stature (defined as Z-score for height smaller than -2 standard deviations (SD)) and failure to thrive were common features (38%), however without significant change over time (Figure 2A). Clustering of anthropometric data by H4 gene or protein region revealed no obvious genotype-phenotype patterns (Figure 2A). The age range of the cohort is between 10 months and 52 years. Interestingly, the oldest individual shows signs of premature aging with greyed, thinning hair and wrinkly skin, looking at least two decades beyond his biological age, which didn’t occur in his parents. Premature aging has also been observed in Rahman syndrome (MIM 617537), caused by pathogenic variants in *H1-4(HIST1H1E)*; MIM

142220).<sup>24</sup> This phenotype appears to be milder in our H4 cohort, however the majority of the individuals are still quite young. One individual died from leukemia stemming from myelodysplasia (P28), but no other individuals were reported to have bone marrow abnormalities.

Non-neurological features were variable across the cohort. Facial features comprised a wide spectrum (Figure 2B). While some individuals were relatively non-dysmorphic, others had a common presentation affecting the facial midline, with hypertelorism (17%), a high nasal bridge (or conversely very low nasal bridge) with a broad nasal base (38%) and narrow nares, wide mouth with a gap between central incisors or other tooth anomalies (21%) (Figure 2C), and moderately pointy chin. Visual impairment such as strabismus, astigmatism, or myopia were reasonably common (61% individuals), and 24% individuals demonstrated hearing impairment. Skeletal development was normal for most individuals, however recurring features such as vertebral or digit abnormalities were present in several individuals (Figure 2D), and particularly severe in individual P28. Variability in clinical features and growth was noted even amongst the seven individuals harboring the same *de novo* variant Arg45Cys in *H4C5* (Figure 2B, Figure S1).

To validate the pathogenic effect of these variants, we expressed wild type human histone H4 and the histone H4 variants pertaining to this study in zebrafish by means of mRNA microinjection (Figure 3). The complete conservation of the zebrafish and human histone H4 proteins at the amino acid sequence level and the early, mRNA-mediated ectopic overexpression make this an optimal set-up for assaying the variants' effect on early development. Early embryonic effects were evaluated at 28 hours post fertilization (hpf) as fundamental developmental processes such as gastrulation and primary organogenesis are then completed. All variants tested displayed significant visible developmental effects compared to microinjection of the corresponding wild type H4 gene, except the Pro32Ala and Arg40Cys variants. Specifically, classification was based on cephalic development, anterior-posterior axis establishment and tissue necrosis during early embryonic

development, as these parameters captured the major defects and the cellular toxicity (Figure 3A,B,C) observed across all variants analyzed. Phenotypic observation revealed that variants affecting Lys91 and His75 caused the strongest effects. Interestingly, these two variants both cluster at the core of the nucleosome, and His75 plays a role in DNA damage repair,<sup>22</sup> a process previously suggested to be involved in the syndromic features of Lys91 individuals.<sup>4</sup> His75 is at the interface between two histone molecules within the octamer (in this case H4 and H2B) and it is located in the *lrs* (loss-of-ribosomal DNA silencing) domain of H4<sup>22</sup>, a nucleosomal surface structure reported to have gene-specific silencing function in yeast<sup>19</sup>. Additionally, we observed a dosage-dependent effect for Arg40His and Arg45Cys (Figure 3D, E), which has been noted for other sprocket arginine substitutions and may relate to possible roles in higher-order organization of chromatin.<sup>25</sup> Interestingly, such sprocket function has been reported for both the *sin* (switch-independent) and *lrs* H4 domains containing Arg45 and His75, respectively.<sup>26</sup> These regions have an almost identical three-dimensional structure<sup>26</sup> and play a role in gene regulation (repression), the perturbation of which likely results in pathogenicity, and was detected in our functional assay. The variability in frequency of phenotype occurrence across variants may reflect the importance of the affected residues in cellular processes crucial to active cell proliferation, as the early zebrafish embryo is a system in which cells have a relatively short cell cycle time. The milder effect observed in our functional assay for variants affecting Pro32 and Arg40 may point to a moderate requirement, however the strong recurrence of variants affecting these residues in our cohort provides alternative evidence to support their pathogenicity. Altogether, these results provide a first picture of the variety of phenotypes caused by the assayed variants, supporting our genetic data. However, as their interpretation is limited by their transience and the inherent variability of our current mRNA assay, further testing in a stable model is required to get more insight in the molecular mechanisms linking genetic variants and phenotype.

Through genetic and developmental findings, we have identified pathogenic substitutions in six genes encoding histone H4 in a large cohort of individuals with a neurodevelopmental syndrome. Despite well-established cellular requirements for post-translational modification of the N-terminal tail of H4<sup>27-29</sup>, it is notable that no *de novo* variants were identified in this region.

Recently, a large cohort of individuals with a neurodegenerative and developmental disorder were reported harbouring *de novo* missense variants in the histone H3 replication-independent genes, *H3F3A* (MIM 601128) and *H3F3B* (MIM 601058).<sup>23</sup> While there are phenotypic commonalities between the H3.3 cohort and individuals presented here, the presentations are distinct. The H3F3A/H3F3B cohort appears to have a more expansive neurological dysfunction with anomalies noted on imaging, accompanied by septal or genital abnormalities and craniosynostosis. In contrast, our H4 cohort has ID/DD and microcephaly as presenting features, but only more rarely are there other neurodevelopmental abnormalities. The pathogenic variants identified in *H3F3A* and *H3F3B* are located throughout the protein, with a smaller number of recurrently occurring variants. In comparison, for histone H4, the high level of recurrent variants observed is significant, along with the clear clustering of the variants in two regions of the H4 protein.

The redundancy of the H4 genes in the human genome is remarkable. Loss-of-function variants in H4 genes are present in the healthy population,<sup>17</sup> and are even present in homozygous form,<sup>30</sup> supporting our hypothesis that the variants identified here act through a dominant effect. This disease mechanism, combined with the paralogous landscape of H4 genes, presents opportunities for future treatment strategies through targeted knockdown of specific H4 gene products.

## Acknowledgements

The authors thank all individuals and their families who were involved in this study, Anisha Chopra for experimental work, and Jacques Giltay, Meriel McEntagart and Cynthia Morton for advice. FT is supported by NWO grant NWO/OCENW.GROOT.2019.029, AOMW was supported by the NIHR Oxford Biomedical Research Centre, KK and LSB were supported by the Marsden Fund, and LSB was supported by a Rutherford Discovery Fellowship, both administered by the Royal Society of New Zealand. AODL is supported by a Manton Endowed Scholar Award. Project support was provided by Fondazione Bambino Gesù (Vite Coraggiose), Italian Ministry of Health (5x1000, CCR-2017-23669081 and RCR-2020-23670068\_001), Italian Ministry of Research (FOE 2019), and the Cliff Broad Family Trust, administered by the Neurological Foundation of New Zealand.

The opinions expressed here are those of the authors and do not reflect those of the Navy, the Department of Defense or the United States government.

The DDD study presents independent research commissioned by the Health Innovation Challenge Fund (grant HICF-1009-003), a parallel funding partnership between the Wellcome Trust with the Department of Health and the Wellcome Trust Sanger Institute (grant WT098051). The views expressed in this publication are those of the author(s) and not necessarily those of the Wellcome Trust or the Department of Health. The study has UK Research Ethics Committee approval (10/H0305/83, granted by the Cambridge South REC, and GEN/284/12, granted by the Republic of Ireland REC). The research team acknowledges the support of the National Institute for Health Research, through the Comprehensive Clinical Research Network.

## Author Contributions

LSB and GvH identified and recruited the study subjects. LSB collated the clinical information. FT, LSB and GvH designed the study. KD performed molecular cloning. KK, MF



and PM performed the structural modelling. FT, JB and GvH designed zebrafish experiments. FT carried out the zebrafish experiments. All other authors assisted with genetic and clinical information for affected individuals. FT, LSB and GvH wrote the manuscript. All authors approved the final manuscript.

#### **Web Resources**

Online Mendelian Inheritance in Man: <https://omim.org/>

#### **Data and Code Availability**

Full genetic data is not available due to privacy regulations.

#### **Declaration of Interests**

The authors declare no competing interests.

**Figure 1. H4 variants identified in the cohort. (A)** Highly recurrent variants were found in six different H4 genes (*H4C3*, *H4C4*, *H4C5*, *H4C6*, *H4C9* and *H4C11*), which all encode an identical protein. Aggregate prevalence of disease-causing amino acid changes is also shown. The N-terminal methionine is cleaved from histone H4, therefore all numbering is relative to the mature polypeptide, in keeping with the protein literature. **(B)** The affected residues of H4 (orange ribbon) either cluster to the N-terminal  $\alpha$ -helix facing towards DNA (Cluster 1, purple spheres), or are located in regions buried within the nucleosome core (Cluster 2, orange spheres). Size of sphere indicates the relative prevalence of substitutions affecting that residue.

**Figure 2. Clinical characteristics of individuals with histone H4 gene variants.**

**(A)** Individuals with variants in histone H4 genes demonstrate a reduction in height, weight and brain growth (OFC, occipitofrontal circumference), with the latter significantly progressing as the individuals age. There are no detectable genotype-phenotype patterns separating by the specific histone H4 gene or variant cluster. \*\*\*\*  $P < 0.0001$ . **(B)** Facial dysmorphism affecting midline structures is noticeable amongst the cohort, but highly variable, with no obvious genotype-phenotype correlation. **(C)** Individuals can present with abnormalities in the appearance and position of teeth (for example, P5, P25). A recurring feature present in several individuals is a noticeable gap between the upper central incisors. **(D)** Individuals with variants in histone H4 genes also show a spectrum of toe anomalies, ranging from no anomalies present (for example P21) through to severe 2-3 toe (P1, P28) or 3-4 toe (P25) syndactyly, which can be bilateral. Toes can also be short (P19, P28).

**Figure 3. H4 variants induce developmental defects in zebrafish embryos. (A)**

Phenotypical characterization in 28 hpf embryos. Representative images of observed phenotypes in zebrafish embryos 28 hr post-fertilization microinjected with mRNA encoding either wild-type or identified variants at the one-cell stage. The different classes are defined on general development and necrosis. **(B)** and **(C)** Detailed view of cephalic necrosis (B) and curved tail (C) phenotypes. **(D)** and **(E)** Quantification of the phenotypical classification as described in (A). Variants reported in (D) were microinjected with 50 pg/embryo, additional testing with 100 pg/embryo is reported in (E). Data marked with a hash symbol was previously published in <sup>4</sup>. Fisher's exact test: ns: not significant,  $P>0.05$ ; \* $P<0.05$ ; \*\*\*\* $P<0.0001$ : Scale bars: (A): 100  $\mu\text{m}$ ; (B,C): 50  $\mu\text{m}$ .

378 **Table 1. Variants identified in H4 genes.**

Number of individuals	Gene	Chromosomal position (hg38)	cDNA	Protein	H4# numbering	CADD PHRED	REVEL score
1	<i>H4C3</i>	6:26104044	c.97C>G	p.(Pro33Ala)	Pro32Ala	23.1	0.526
2	<i>H4C3</i>	6:26104045	c.98C>T	p.(Pro33Leu)	Pro32Leu	25.7	0.438
3	<i>H4C3</i>	6:26104221	c.274A>C	p.(Lys92Gln)	Lys91Gln	26.6	0.706
1	<i>H4C4</i>	6:26188955	c.122G>A	p.(Arg41His)	Arg40His	23.9	0.459
1	<i>H4C5</i>	6:26204739	c.95A>C	p.(Lys32Thr)	Lys31Thr	26.6	0.523
1	<i>H4C5</i>	6:26204742	c.98C>G	p.(Pro33Arg)	Pro32Arg	25.3	0.541
1	<i>H4C5</i>	6:26204750	c.106C>T	p.(Arg36Trp)	Arg35Trp	26.6	0.494
1	<i>H4C5</i>	6:26204757	c.113T>C	p.(Leu38Pro)	Leu37Pro	27.5	0.659
4	<i>H4C5</i>	6:26204765	c.121C>T	p.(Arg41Cys)	Arg40Cys	26.6	0.446
7	<i>H4C5</i>	6:26204780	c.136C>T	p.(Arg46Cys)	Arg45Cys	26.3	0.589
2	<i>H4C5</i>	6:26204939	c.295T>C	p.(Tyr99His)	Tyr98His	26.9	0.317
1	<i>H4C6</i>	6:26240708	c.283G>A	p.(Gly95Arg)	Gly94Arg	24.5	0.677
1	<i>H4C9</i>	6:27139430	c.122G>T	p.(Arg41Leu)	Arg40Leu	26.7	0.628
2	<i>H4C9</i>	6:27139535	c.227A>G	p.(His76Arg)	His75Arg	25.3	0.754
1	<i>H4C11</i>	6:27824245	c.121C>T	p.(Arg41Cys)	Arg40Cys	25.8	0.541

379 RefSeq IDs: *H4C3*: NM\_003542.4, *H4C4*: NM\_003539.4, *H4C5*: NM\_003545.3, *H4C6*: NM\_003540.4, *H4C9*: NM\_003495.2, *H4C11*:  
380 NM\_021968.4. # Note on Nomenclature: To refer to the residues belonging to this study, HGVS Variant nomenclature would include  
381 Methionine-1 (Met1) at the translation initiating site (e.g. *H4C3* Pro33Ala [c.97C>G; p.(Pro33Ala)]. However, as the research field of epigenetics  
382 and oncohistones typically drops this first post-translationally removed methionine, we have also done so. Therefore, the above-mentioned  
383 example (included in this study) is referred to as *H4C3* Pro32Ala.

**Table 2: Clinical features of individuals in the H4 cohort**

<b>Clinical Feature</b>	<b>Proportion (percentage)</b>
<b>Neurodevelopment</b>	
Intellectual Disability	29/29 (100%)
Developmental Delay	29/29 (100%)
Hypotonia	10/29 (34%)
Seizures	5/29 (17%)
Autism	5/29 (17%)
Ataxia	4/29 (14%)
<b>Growth</b>	
Microcephaly - prenatal onset	2/19 (11%)
- postnatal	20/29 (69%)
Short stature	11/29 (38%)
Failure to thrive	11/29 (38%)
<b>Skeletal Features</b>	
Craniosynostosis	2/29 (7%)
Digit anomalies	4/29 (14%)
Vertebral anomalies	4/27 (15%)
<b>Facial features</b>	
Hypertelorism	5/29 (17%)
Upslanting palpebral fissures	3/29 (10%)
Broad nasal tip	11/29 (38%)
Thin upper lip / vermillion	4/29 (14%)
Teeth anomalies	6/29 (21%)
<b>Other features</b>	
Recurrent infections	4/29 (14%)
Visual impairment	17/28 (61%)
Hearing impairment	7/29 (24%)
Age range	10m – 52 y (median 10 y 11 m)

Y – year, m – months.

## References

1. Kamakaka, R.T., and Biggins, S. (2005). Histone variants: deviants? *Genes Dev* *19*, 295-310. 10.1101/gad.1272805.
2. Pusarla, R.H., and Bhargava, P. (2005). Histones in functional diversification. Core histone variants. *FEBS J* *272*, 5149-5168. 10.1111/j.1742-4658.2005.04930.x.
3. Ye, J., Ai, X., Eugeni, E.E., Zhang, L., Carpenter, L.R., Jelinek, M.A., Freitas, M.A., and Parthun, M.R. (2005). Histone H4 lysine 91 acetylation a core domain modification associated with chromatin assembly. *Mol Cell* *18*, 123-130. 10.1016/j.molcel.2005.02.031.
4. Tessadori, F., Giltay, J.C., Hurst, J.A., Massink, M.P., Duran, K., Vos, H.R., van Es, R.M., Deciphering Developmental Disorders, S., Scott, R.H., van Gassen, K.L.I., et al. (2017). Germline mutations affecting the histone H4 core cause a developmental syndrome by altering DNA damage response and cell cycle control. *Nat Genet* *49*, 1642-1646. 10.1038/ng.3956.
5. Tessadori, F., Rehman, A.U., Giltay, J.C., Xia, F., Streff, H., Duran, K., Bakkers, J., Lalani, S.R., and van Haaften, G. (2020). A de novo variant in the human HIST1H4J gene causes a syndrome analogous to the HIST1H4C-associated neurodevelopmental disorder. *Eur J Hum Genet* *28*, 674-678. 10.1038/s41431-019-0552-9.
6. Yan, Q., Dutt, S., Xu, R., Graves, K., Juszczynski, P., Manis, J.P., and Shipp, M.A. (2009). BBAP monoubiquitylates histone H4 at lysine 91 and selectively modulates the DNA damage response. *Mol Cell* *36*, 110-120. 10.1016/j.molcel.2009.08.019.
7. Bagert, J.D., Mitchener, M.M., Patriotis, A.L., Dul, B.E., Wojcik, F., Nacev, B.A., Feng, L., Allis, C.D., and Muir, T.W. (2021). Oncohistone mutations enhance chromatin remodeling and alter cell fates. *Nat Chem Biol* *17*, 403-411. 10.1038/s41589-021-00738-1.
8. Nacev, B.A., Feng, L., Bagert, J.D., Lemiesz, A.E., Gao, J., Soshnev, A.A., Kundra, R., Schultz, N., Muir, T.W., and Allis, C.D. (2019). The expanding landscape of 'oncohistone' mutations in human cancers. *Nature* *567*, 473-478. 10.1038/s41586-019-1038-1.
9. Lewis, P.W., Muller, M.M., Koletsky, M.S., Cordero, F., Lin, S., Banaszynski, L.A., Garcia, B.A., Muir, T.W., Becher, O.J., and Allis, C.D. (2013). Inhibition of PRC2 activity by a gain-of-function H3 mutation found in pediatric glioblastoma. *Science* *340*, 857-861. 10.1126/science.1232245.
10. Lu, C., Jain, S.U., Hoelper, D., Bechet, D., Molden, R.C., Ran, L., Murphy, D., Venneti, S., Hameed, M., Pawel, B.R., et al. (2016). Histone H3K36 mutations promote sarcomagenesis through altered histone methylation landscape. *Science* *352*, 844-849. 10.1126/science.aac7272.
11. Papillon-Cavanagh, S., Lu, C., Gayden, T., Mikael, L.G., Bechet, D., Karamboulas, C., Ailles, L., Karamchandani, J., Marchione, D.M., Garcia, B.A., et al. (2017). Impaired H3K36 methylation defines a subset of head and neck squamous cell carcinomas. *Nat Genet* *49*, 180-185. 10.1038/ng.3757.
12. Tropberger, P., and Schneider, R. (2013). Scratching the (lateral) surface of chromatin regulation by histone modifications. *Nat Struct Mol Biol* *20*, 657-661. 10.1038/nsmb.2581.

13. Sobreira, N., Schiettecatte, F., Valle, D., and Hamosh, A. (2015). GeneMatcher: a matching tool for connecting investigators with an interest in the same gene. *Hum Mutat* 36, 928-930. 10.1002/humu.22844.
14. Firth, H.V., Richards, S.M., Bevan, A.P., Clayton, S., Corpas, M., Rajan, D., Van Vooren, S., Moreau, Y., Pettett, R.M., and Carter, N.P. (2009). DECIPHER: Database of Chromosomal Imbalance and Phenotype in Humans Using Ensembl Resources. *Am J Hum Genet* 84, 524-533. 10.1016/j.ajhg.2009.03.010.
15. Miller, J.A., Ding, S.L., Sunkin, S.M., Smith, K.A., Ng, L., Szafer, A., Ebbert, A., Riley, Z.L., Royall, J.J., Aiona, K., et al. (2014). Transcriptional landscape of the prenatal human brain. *Nature* 508, 199-206. 10.1038/nature13185.
16. Pollen, A.A., Nowakowski, T.J., Chen, J., Retallack, H., Sandoval-Espinosa, C., Nicholas, C.R., Shuga, J., Liu, S.J., Oldham, M.C., Diaz, A., et al. (2015). Molecular identity of human outer radial glia during cortical development. *Cell* 163, 55-67. 10.1016/j.cell.2015.09.004.
17. Karczewski, K.J., Francioli, L.C., Tiao, G., Cummings, B.B., Alfoldi, J., Wang, Q., Collins, R.L., Laricchia, K.M., Ganna, A., Birnbaum, D.P., et al. (2020). The mutation/variant constraint spectrum quantified from variation in 141,456 humans. *Nature* 581, 434-443. 10.1038/s41586-020-2308-7.
18. Tessarz, P., and Kouzarides, T. (2014). Histone core modifications regulating nucleosome structure and dynamics. *Nat Rev Mol Cell Biol* 15, 703-708. 10.1038/nrm3890.
19. Kruger, W., Peterson, C.L., Sil, A., Coburn, C., Arents, G., Moudrianakis, E.N., and Herskowitz, I. (1995). Amino acid substitutions in the structured domains of histones H3 and H4 partially relieve the requirement of the yeast SWI/SNF complex for transcription. *Genes Dev* 9, 2770-2779. 10.1101/gad.9.22.2770.
20. Luger, K., Mader, A.W., Richmond, R.K., Sargent, D.F., and Richmond, T.J. (1997). Crystal structure of the nucleosome core particle at 2.8 Å resolution. *Nature* 389, 251-260. 10.1038/38444.
21. Chavez, M.S., Scorgie, J.K., Dennehey, B.K., Noone, S., Tyler, J.K., and Churchill, M.E. (2012). The conformational flexibility of the C-terminus of histone H4 promotes histone octamer and nucleosome stability and yeast viability. *Epigenetics Chromatin* 5, 5. 10.1186/1756-8935-5-5.
22. Selvam, K., Rahman, S.A., and Li, S. (2019). Histone H4 H75E mutation attenuates global genomic and Rad26-independent transcription-coupled nucleotide excision repair. *Nucleic Acids Res* 47, 7392-7401. 10.1093/nar/gkz453.
23. Bryant, L., Li, D., Cox, S.G., Marchione, D., Joiner, E.F., Wilson, K., Janssen, K., Lee, P., March, M.E., Nair, D., et al. (2020). Histone H3.3 beyond cancer: Germline mutations in Histone 3 Family 3A and 3B cause a previously unidentified neurodegenerative disorder in 46 patients. *Sci Adv* 6. 10.1126/sciadv.abc9207.
24. Flex, E., Martinelli, S., Van Dijck, A., Ciolfi, A., Cecchetti, S., Coluzzi, E., Pannone, L., Andreoli, C., Radio, F.C., Pizzi, S., et al. (2019). Aberrant Function of the C-Terminal Tail of HIST1H1E Accelerates Cellular Senescence and Causes Premature Aging. *Am J Hum Genet* 105, 493-508. 10.1016/j.ajhg.2019.07.007.
25. Hodges, A.J., Gallegos, I.J., Laughery, M.F., Meas, R., Tran, L., and Wyrick, J.J. (2015). Histone Sprocket Arginine Residues Are Important for Gene Expression, DNA Repair, and Cell Viability in *Saccharomyces cerevisiae*. *Genetics* 200, 795-806. 10.1534/genetics.115.175885.
26. Park, J.H., Cosgrove, M.S., Youngman, E., Wolberger, C., and Boeke, J.D. (2002). A core nucleosome surface crucial for transcriptional silencing. *Nat Genet* 32, 273-279. 10.1038/ng982.



27. Sanders, S.L., Portoso, M., Mata, J., Bahler, J., Allshire, R.C., and Kouzarides, T. (2004). Methylation of histone H4 lysine 20 controls recruitment of Crb2 to sites of DNA damage. *Cell* *119*, 603-614. 10.1016/j.cell.2004.11.009.
28. Shogren-Knaak, M., Ishii, H., Sun, J.M., Pazin, M.J., Davie, J.R., and Peterson, C.L. (2006). Histone H4-K16 acetylation controls chromatin structure and protein interactions. *Science* *311*, 844-847. 10.1126/science.1124000.
29. Schotta, G., Lachner, M., Sarma, K., Ebert, A., Sengupta, R., Reuter, G., Reinberg, D., and Jenuwein, T. (2004). A silencing pathway to induce H3-K9 and H4-K20 trimethylation at constitutive heterochromatin. *Genes Dev* *18*, 1251-1262. 10.1101/gad.300704.
30. DeBoever, C., Tanigawa, Y., Lindholm, M.E., McInnes, G., Lavertu, A., Ingelsson, E., Chang, C., Ashley, E.A., Bustamante, C.D., Daly, M.J., and Rivas, M.A. (2018). Medical relevance of protein-truncating variants across 337,205 individuals in the UK Biobank study. *Nat Commun* *9*, 1612. 10.1038/s41467-018-03910-9.

Figure 1  
Figure 1.

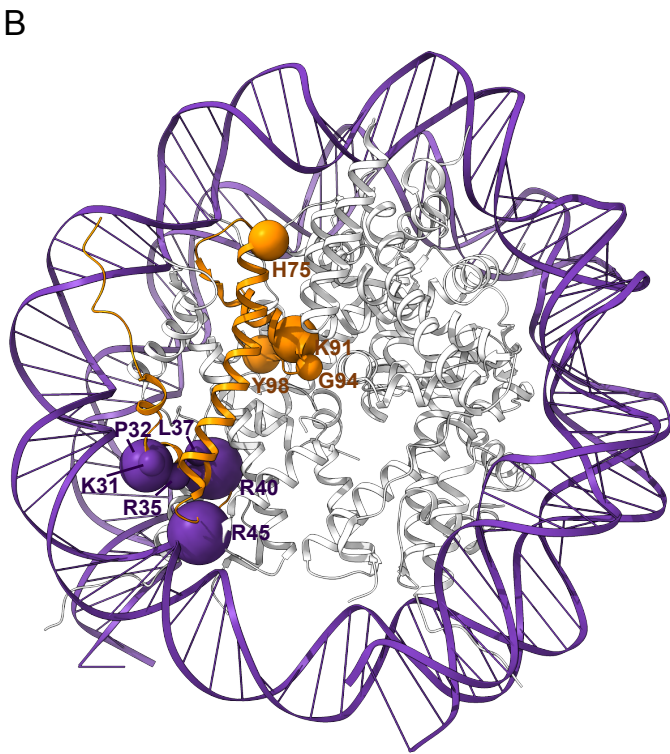
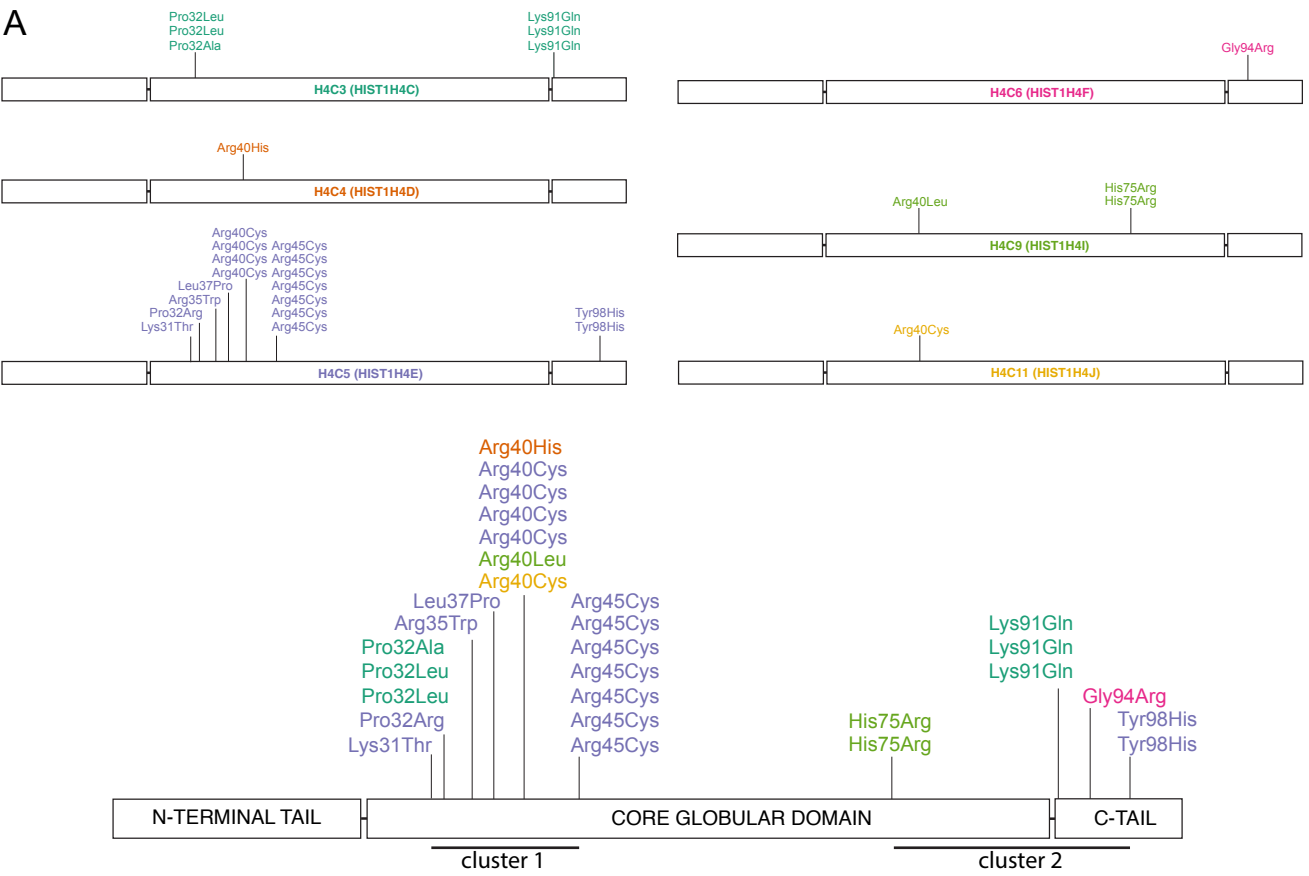
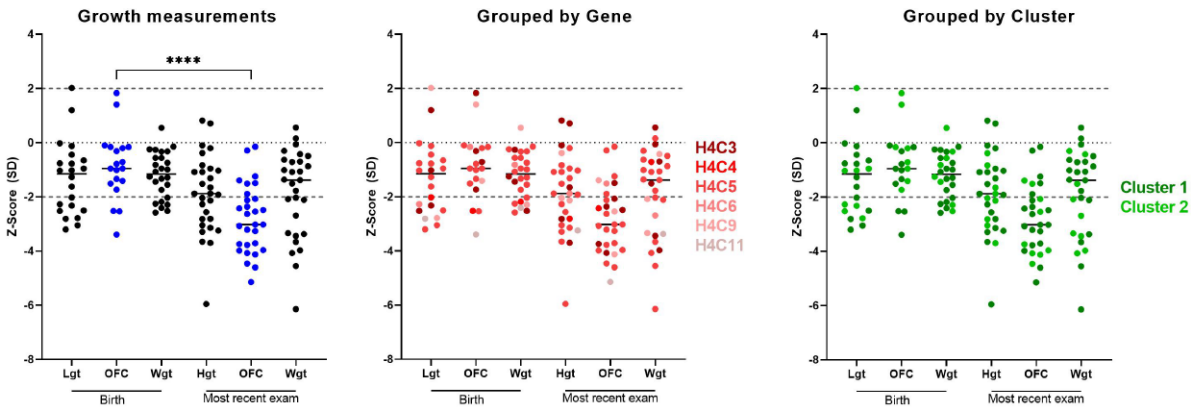


Figure 2

Figure 2

A



B



C



D

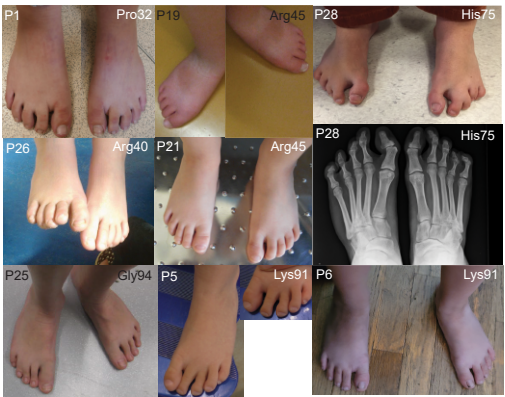
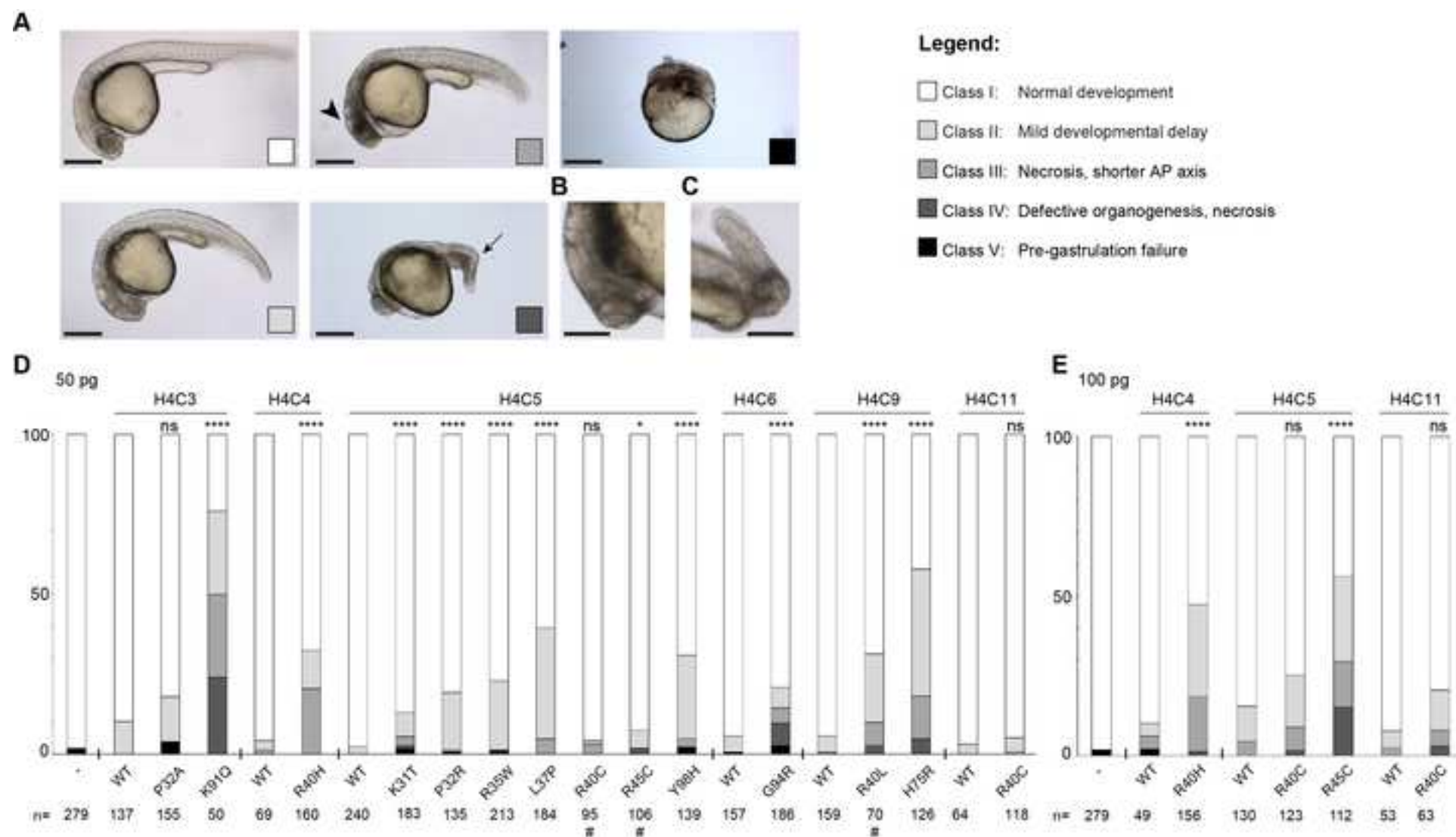
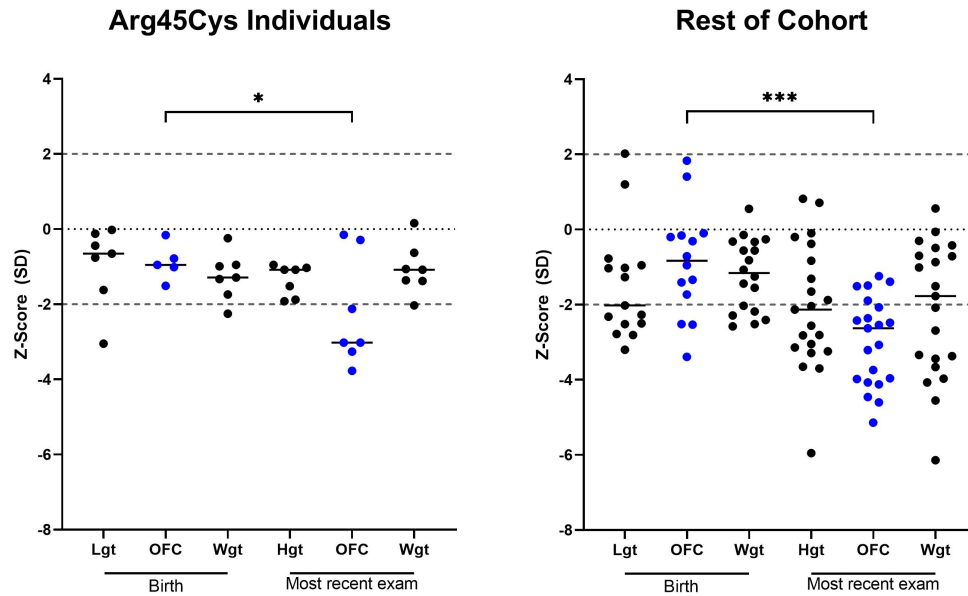


Figure 3

[Click here to access/download;Figure;Figure 3.jpg](#)



**Figure S1. Variability in growth parameters in individuals with the Arg45Cys variant.**

Growth parameters of individuals with the most common recurring variant Arg45Cys highlight the variability observed across the cohort, especially in OFC changes as the individuals age. One-way ANOVA, allowing for multiple comparisons; \*  $p = 0.041$ , \*\*\*  $p = 0.0002$ . OFC, occipitofrontal circumference.



a



b

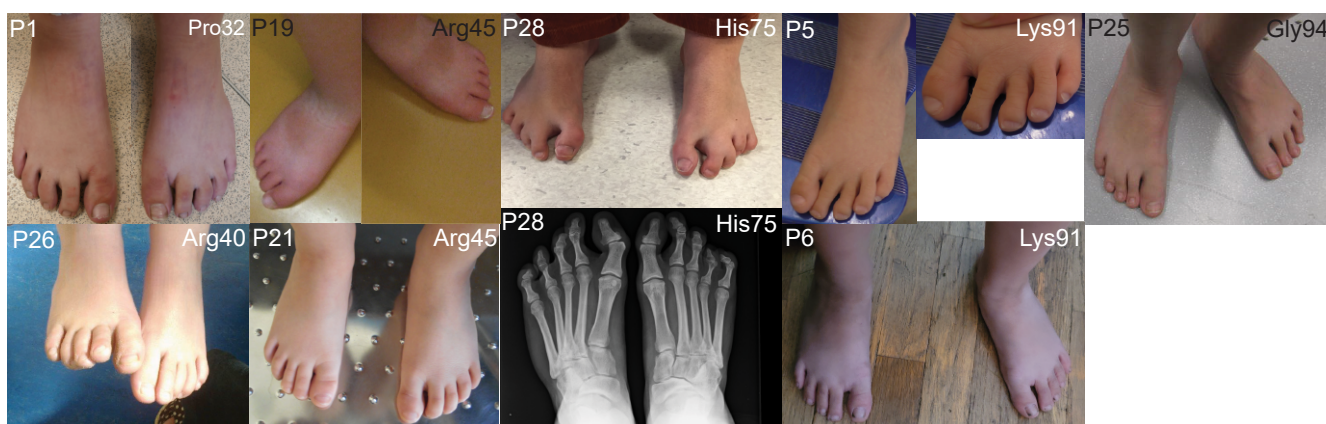


**Figure S2.** Clinical observations in the histone H4 patient cohort.

(a) Individuals can present with abnormalities in the appearance and position of teeth (for example, P5, P24). A recurring feature present in several individuals is a noticeable gap between the upper central incisors.

(b) Individuals with variants in histone H4 genes also show a spectrum of toe anomalies, ranging from no anomalies present (for example P20) through to severe 2-3 toe (P1, P27) or 3-4 toe (P24) syndactyly, which can be bilateral. Toes can also be short (P18, P27).

Table S2: Oligonucleotide sequences used for cloning and site-directed mutagenesis.

Gene	Variant	Name	Sequence	Purpose
H4C3 (HIST1H4C)	WT	Hist1H4C_FL_F Hist1H4C_FL_R	5'-GCCACCATGTCTGGTCGCGGCAAAG-3' 5'-TCAGCCGCCGAAGCCATAC-3'	cDNA amplification
	Pro32Ala	Hist1H4C_P32A_F Hist1H4C_P32A_R	5'-ACATCCAGGGCATTACAAAAGCGGCTATTTCGCC-3' 5'-GGCGAATAGCCGCTTTTGTAAATGCCCTGGATGT-3'	Site-directed mutagenesis
H4C4 (HIST1H4D)	WT	Hist1H4D_FL_F Hist1H4D_FL_R	5'-GCCACCATGTCTGGCCGCGGTAAGGG-3' 5'-TCAGCCGCCGAAGCCATAAAG-3'	cDNA amplification
	Arg40His	Hist1H4D_R40H_F Hist1H4D_R40H_R	5'-CCTGGCTCGCCACGGCGGCGTCA-3' 5'-TGACGCCGCCGTGGCGAGCCAGG-3'	Site-directed mutagenesis
H4C5 (HIST1H4E)	WT	Hist1H4E_FL_F Hist1H4E_FL_R	5'-GCCACCATGTCTGGTCGCGGCAAAGGC-3' 5'-TTAGCCGCCGAAGCCGTAAG-3'	cDNA amplification
	Lys31Thr	Hist1H4E_K31T_F Hist1H4E_K31_R	5'-ATAACATCCAGGGCATTACCACGCCTGCCATCC-3' 5'-GGATGGCAGGCGTGGTAATGCCCTGGATGTTAT-3'	Site-directed mutagenesis
	Pro32Arg	Hist1H4E_P32R_F Hist1H4E_P32R_R	5'-GGCATTACCAAGCGTGCCATCCGGCGC-3' 5'-GCGCCGGATGGCAGCCTTGGTAATGCC-3'	Site-directed mutagenesis
	Arg35Trp	Hist1H4E_R35W_F Hist1H4E_R35W_R	5'-CAAGCCTGCCATCTGGCGCCTTGCTCG-3' 5'-CGAGCAAGGCGCCAGATGGCAGGCTTG-3'	Site-directed mutagenesis
	Leu37Pro	Hist1H4E_L37P_F Hist1H4E_L37P_R	5'-CATCCGGCGCCCTGCTCGTCGCG-3' 5'-CGCGACGAGCAGGGCGCCGGATG-3'	Site-directed mutagenesis
	Tyr98His	Hist1H4E_Y98H_F Hist1H4E_Y98H_R	5'-GACAGGGACGCACTCTTCACGGCTTCGGC-3' 5'-GCCGAAGCCGTGAAGAGTGCGTCCCTGTC-3'	Site-directed mutagenesis
H4C6 (HIST1H4F)	WT	Hist1H4F_FL_F Hist1H4F_FL_R	5'-GCCACCATGTCTGGTAGAGGCAAAGGTG-3' 5'-TCAGCCACCAAAGCCGTACAG-3'	cDNA amplification
	Gly94Arg	Hist1H4F_G94R_F Hist1H4F_G94R_R	5'-CGCTCAAGCGCCAGAGACGCACTCTGTAC-3' 5'-GTACAGAGTGCGTCTCTGGCGCTTGAGCG-3'	Site-directed mutagenesis
H4C9 (HIST1H4I)	WT	Hist1H4I_FL_F Hist1H4I_FL_R	5'-GCCACCATGTCAGGACGCGGCAAAGGA-3' 5'-TTAGCCGCCGAAGCCATAGAG-3'	cDNA amplification
	His75Arg	Hist1H4I_H75R_F Hist1H4I_H75R_R	5'-ACCTACACGGAGCGCGCCAAGCGCAAG-3' 5'-CTTGCGCTTGGCGCGCTCCGTGTAGGT-3'	Site-directed mutagenesis
H4C11 (HIST1H4J)	WT	Hist1H4J_FL_F Hist1H4J_FL_R	5'-GCCACCATGTCTGGCCGCGGCAAAGGC-3' 5'-TAGGGTGGCCCTGAAAAGGGCC-3'	cDNA amplification
	Arg40Cys	Hist1H4J_R40C_F Hist1H4J_R40C_R	5'-GCCTTGCTCGCTGCGGCGGCGTG-3' 5'-CACGCCGCCGAGCGAGCAAGGC-3'	Site-directed mutagenesis

Table S3: Source data from the zebrafish RNA injection experiments at 50 pg, used to generate Fig 3D.

	No injection	H4C3 WT	H4C3 P32A	H4C3 K91Q	H4C4 WT	H4C4 R40H	H4C5 WT	H4C5 K31T	H4C5 P32R	H4C5 R36W	H4C5 L37P	H4C5 R40C	H4C5 R45C	H4C5 Y98H	H4C6 WT	H4C6 G94R	H4C9 WT	H4C9 R40L	H4C9 H75R	H4C11 WT	H4C11 R40C
Class I	273	123	127	12	66	108	234	159	109	164	111	91	98	96	148	147	150	48	53	62	112
Class II	1	14	22	13	2	19	6	14	24	46	64	1	6	36	8	12	8	15	50	2	5
Class III	0	0	0	13	1	33	0	5	1	1	9	3	0	4	0	9	1	5	17	0	1
Class IV	0	0	0	12	0	0	0	2	0	0	0	0	2	0	0	13	0	2	6	0	0
Class V	5	0	6	0	0	0	0	3	1	2	0	0	0	3	1	5	0	0	0	0	0
Total	279	137	155	50	69	160	240	183	135	213	184	95	106	139	157	186	159	70	126	64	118

Table S4: Source data from the zebrafish RNA injection experiments at 100 pg, used to generate Fig 3E.

	No injection	H4C4 WT	H4C4 R40H	H4C5 WT	H4C5 R40C	H4C5 R45C	H4C11 WT	H4C11 R40C
Class I	273	44	82	110	92	49	36	50
Class II	1	2	45	14	20	30	2	8
Class III	0	2	27	6	9	16	1	3
Class IV	0	0	2	0	2	17	0	2
Class V	5	1	0	0	0	0	0	0
Total	279	49	156	130	123	112	39	63



## **Supplemental Methods**

### **Patient Recruitment**

Exome sequencing was undertaken for either research or clinical genetic testing, using standard pipelines at each referring centre. *De novo* status was confirmed by either trio-based exome sequencing and/or Sanger sequencing. Growth measurements were converted to Z-scores using the LSMgrowth method<sup>1</sup> or the Fenton 2013 growth chart<sup>2</sup> for preterm births.

### **Protein Modelling**

Variants were visualised on the human nucleosome structure (PDB code 5y0c<sup>3</sup>) using UCSF Chimera<sup>4</sup>.

### **Fish lines and husbandry**

Zebrafish (*Danio rerio*) of the Tübingen longfin strain were kept in standard laboratory conditions<sup>5</sup>. Animal experiments were approved by the Animal Experimentation Committee of the Royal Netherlands Academy of Arts and Sciences.

### **Expression assay in zebrafish embryos**

Capped mRNA microinjections were carried out essentially as described<sup>6</sup>. Template human cDNA (H4C3, H4C4, H4C5, H4C6, H4C9 and H4C11) was used to generate novel cDNA encoding respectively H4C3 Pro32Ala, H4C4 Arg40His, H4C5 Leu37Pro, H4C5 Tyr98His, H4C5 Pro32Arg, H4C5 Arg35Trp, H4C6 Gly94Arg, H4C9 His75Arg and H4C11 Arg40Cys using oligonucleotides listed in Table S2. After cloning into pCS2GW by Gateway cloning (Life Technologies), the resulting template constructs were linearized with NotI-HF (New England BioLabs) and used for *in vitro* synthesis of capped mRNA with MESSAGE mMACHINE SP6 Ultra kit (Life Technologies). Microinjections in 1-cell-stage embryos were carried out with 50 pg or 100 pg of mRNA per embryo. After microinjection embryos were kept at 28.5 °C in E3 medium and development was assessed at approximately 28 hours post-fertilization. Phenotypical assessment data was collected for each histone variant over a minimum of two independent microinjection rounds.

## Imaging

Live observation of 28 hpf zebrafish embryos was carried out on a Zeiss StemiSV6 stereomicroscope (Carl Zeiss AG, Oberkochen, Germany). Image capture was performed with a Leica DFC420C digital microscope camera (Leica Microsystems, Wetzlar, Germany) mounted on a Zeiss Axioplan brightfield microscope (Carl Zeiss AG).

## Statistics

Statistics analysis was carried out with Prism 9 (Graphpad). Fisher's exact test was carried out on each histone H4 variant and the corresponding wild type. To carry out Fisher's test, we classified the scored phenotypes in only two outcomes: "no phenotype" (Class I) and "presence of a phenotype" (Class II + Class III + Class IV + Class V). The *P* values, levels of significance and number of embryos analyzed are reported in the figure and the figure legend. The source data used to generate figures 3D and E are shown in Tables S3 and S4, respectively.

## Supplemental References

1. Cole, T.J. The LMS method for constructing normalized growth standards. *Eur J Clin Nutr* **44**, 45-60 (1990).
2. Fenton, T.R. *et al.* Validating the weight gain of preterm infants between the reference growth curve of the fetus and the term infant. *BMC Pediatr* **13**, 92 (2013).
3. Arimura, Y. *et al.* Cancer-associated mutations of histones H2B, H3.1 and H2A.Z.1 affect the structure and stability of the nucleosome. *Nucleic Acids Res* **46**, 10007-10018 (2018).
4. Pettersen, E.F. *et al.* UCSF Chimera--a visualization system for exploratory research and analysis. *J Comput Chem* **25**, 1605-12 (2004).
5. Alestrom, P. *et al.* Zebrafish: Housing and husbandry recommendations. *Lab Anim* **54**, 213-224 (2020).
6. Tessadori, F. *et al.* Germline mutations affecting the histone H4 core cause a developmental syndrome by altering DNA damage response and cell cycle control. *Nat Genet* **49**, 1642-1646 (2017).